ARTICLES

Imbibition and Flow of Wetting Liquids in Noncircular Capillaries

Enoch Kim and George M. Whitesides*

Department of Chemistry, Harvard University, 12 Oxford Street, Cambridge, Massachusetts 02138

Received: May 31, 1996; In Final Form: September 19, 1996[⊗]

Micromolding in capillaries (MIMIC) has been used to study the dynamics of imbibition of liquid prepolymers in micrometer-scale, rectangular capillaries formed between an elastomer containing relief structures and a self-assembled monolayer (SAM) of alkanethiolates on gold supported on Si/SiO_2. Self-assembled monolayers provide a wide range of solid/vapor interfacial free energies (γ_{SV}) and a control over wetting and spreading of liquids in the capillaries. The dynamic shapes of the liquids in the capillaries are obtained as solid polymers cross-linked photochemically and examined using scanning electron and atomic force microscopies. The shape of the imbibing liquid on a surface with high γ_{SV} shows that precursor structures precede macroscopic flow; on low γ_{SV}, these precursor structures are absent. Rates of capillary imbibition are linearly correlated to the cosine of static advancing contact angles (θ_a) of a liquid prepolymer on different SAMs. Different regimes of spreading are observed on a surface having constant, low γ_{SV}; in regions close to the origin, the liquid spreads with low θ_a and via precursor structures. As the distance relative to the origin increases, the liquid spreads with higher θ_a and the dynamic θ_a approaches static θ_a.

Introduction

The dynamics of wetting and spreading of liquids in capillaries[1−3] are important in many aspects of surface, colloid, and interfacial sciences. Examples include wetting of powders,[4] oil recovery,[5] dispersion of pigments,[6] formation of emulsions,[7] and use of surfactants.[8] The flow of a liquid in a capillary occurs because of a pressure difference between two hydraulically connected regions of the liquid mass, and the direction of flow is such as to decrease this difference in pressure. In circular capillaries, the flow of a wetting liquid occurs initially in thin films that wet the capillary symmetrically. In noncircular capillaries (e.g., capillaries characterizing porous underground media), the most rapid flow occurs in the corner regions. Theories to explain the phenomenon of a wetting liquid imbibing along the corners of noncircular capillaries have been developed extensively[9−11] and confirmed experimentally.[12−14]

In the current study, we have used micromolding in capillaries (MIMIC) to investigate the dynamics of imbibing liquids in rectangular capillaries, and self-assembled monolayers (SAMs) to modify the interfacial properties of the insides of the capillaries and to control the extent of wetting and spreading. We have developed MIMIC primarily as a tool for microfabrication. Examples have included fabrication of microstructures of polymers,[15] patterning of organic and inorganic materials,[16] fabrication and application of microstructured polymeric films,[17] and crystallization of microspheres in micrometer-scale patterns.[18] In MIMIC, we first form an appropriate network of micrometer-scale capillaries by bringing an elastomeric mold (made of poly(dimethylsiloxane), PDMS) containing relief patterns into intimate contact with a solid support. Capillaries formed as a result of this contact are noncircular and have sharp corners. All the work described here was carried out with capillaries having rectangular cross section, although other cross sections are easily fabricated.[19−21] We then allow liquid prepolymers to fill these channels by capillary forces. The shape of the fluid in the capillary can be "frozen" rapidly (∼5−10 s) by using a photopolymerizable prepolymer and irradiating through the optically transparent mold.[22] After the prepolymer has been cured or cross-linked and the shape of the polymer fixed, the elastomeric mold can be removed without destroying this shape. The patterned polymer structures remain on the surface of the support and can be examined and characterized using scanning electron and scanning probe microscopies.

Since the process of MIMIC is based on using interfacial free energies to fill capillaries, it provides an excellent system for observing and studying behaviors of imbibing liquids in capillaries. A number of characteristics of MIMIC make it especially convenient as a technique for analyzing wetting and imbibing of liquids in capillaries. (1) The capillaries have clearly defined shapes that are under the control of the experimenter. The dimensions of these capillaries can be controlled with a lateral edge resolution of ∼100 nm by casting PDMS against photolithographically generated masters.[19,20] (2) The wetting of the solid surfaces by the liquid can be controlled by varying the interfacial free energies of the substrate and/or the mold. This two-component system—the elastomeric mold and the substrate—is the basis of an experimental protocol in which important characteristics of one surface can be modified independently of the other. Patterning the solid surface into regions of different interfacial free energy allows further control over the system. (3) Forming micrometer- and submicrometer-scale capillaries (in linear or complex patterns) is straightforward. (4) A large number of capillary imbibition experiments can be carried out simultaneously, since a PDMS mold typically contains a large number of relief structures, and these structures can have the same or different dimensions. (5) The shape of the imbibing front and the bulk liquid can be preserved using an appropriate liquid prepolymer that can be cross-linked rapidly without the loss of its shape.

* To whom correspondence should be addressed.
[⊗] Abstract published in *Advance ACS Abstracts,* January 1, 1997.

S1089-5647(96)01594-5 CCC: $14.00

Here, we describe the use of MIMIC to study the dynamics of imbibing liquids in rectangular capillaries having micrometer dimensions. This report examines the shapes—observed as cross-linked, solid polymers on the support—of the imbibing fronts on surfaces composed of SAMs having different terminal groups and examines the dependence of the rate of imbibition on the interfacial free energies of and the dynamic contact angles on the surface of the support.

Experimental Section

Materials and Substrates. All experiments were carried out under ambient laboratory conditions (20−26 °C and 25−65% humidity). Thiols were available from the previous study[23] or prepared as described previously.[24] All solvents and chemicals were of reagent quality and used without further purification. Gold (99.999%) was obtained from Materials Research Corp. Hexadecanethiol was obtained from Aldrich and purified by chromatography over silica before use. PDMS (Sylgard 184) was obtained from Dow Corning. Commercially available liquid prepolymers were used: SK-9 (poly(methylacrylate), Summers), UV-15 and UV-15-7 (epoxy, Master Bond), F113 and F114 (epoxy, Tra-Con), J-91 (polyurethane, Summers), and NOA 60, 71, 72, 73, 88, and 113 (Norland). Thin films of gold (500 Å) were prepared by electron-beam evaporation onto silicon wafers (polished single-crystal silicon (test grade, n-doped), Silicon Sense, Nashua, NH) using titanium (10 Å) as an adhesion promoter. Self-assembled monolayers on gold were formed by immersing a gold slide (∼2 cm × 4 cm) in an ethanolic solution of thiol (0.5−1 mM) for 20 min at room temperature. They were rinsed with heptane and ethanol and dried with N_2 before the use. The liquid prepolymers were cross-linked using a Hg vapor lamp (450 W medium pressure, Type 7825-34, ACE Glass).

Instrumentation. Scanning electron microscopy was carried out on a JEOL JSM-6400. Atomic force microscopy was performed using a Topometrix TMX-2010 (Mountain View, CA). The images were obtained in a contact mode, using cantilevers made of silicon nitride.

Contact angles of liquids were measured on a Rame-Hart Model 100 goniometer at room temperature and ambient humidity. A Micro-Electrapette syringe (Matrix Technologies) was used to dispense and remove the liquid from the surface at ∼1 μL/s.

MIMIC. The procedures used in MIMIC have been described previously.[15,16] An elastomeric mold was fabricated from poly(dimethylsiloxane) (PDMS, Sylgard 184, Dow Corning) by casting PDMS against a master (usually prepared by photolithography) that contained a three-dimensional relief pattern to be replicated.[25,26] We reused the master a number of times to fabricate multiple copies of the elastomeric mold. The PDMS mold was made sufficiently thin (approximately 200−500 μm in thickness) to allow efficient transmission[22] of the ultraviolet light. A typical size of the mold varied from ∼0.5 to 4 cm^2 and the length of the channels in the mold from ∼0.5 to 1.5 cm. Both ends of the channels in the mold were open to allow a liquid to enter and air to escape. When the elastomeric mold was placed on the SAMs of alkanethiolates supported on Au/Ti/SiO_2/Si,[27,28] the compliant nature of PDMS allowed close and uninterrupted contact between the mold and the surface, and an array (or a network) of channels formed. These channels were accessible to a fluid from the open end. When a drop (∼0.2−1.0 mL) of a liquid prepolymer was placed at the ends of the channels, the liquid filled the channels by capillary action. After the liquid had filled the channels to the desired distance, it was cross-linked using UV illumination (for 20 min using a medium pressure mercury lamp, 450 W, at 1 cm distance) through the optically transparent PDMS mold. Usually, the outer layer of the liquid prepolymer cross-linked rapidly; after ∼5−10 s, the surface of the polymer was dry to the touch, but the core of the polymer still remained fluid. When the PDMS mold was removed from the support, the patterned polymer adhered preferentially to the surface of the substrate.

Theory

We have explained the thermodynamics of MIMIC in terms of interfacial free energy and a related, experimentally observed phenomenon (i.e., contact angles): a liquid fills capillaries in order to minimize interfacial free energies of solid/vapor and solid/liquid interfaces.[15] MIMIC can be considered a process of capillary displacement in which a liquid that preferentially wets the solid (here, a liquid prepolymer) displaces the one that wets to a lesser extent (here, ambient air). The change in interfacial free energy of capillary filling in MIMIC[15,29] can be approximated in terms of changes in the interfacial (liquid/PDMS and liquid/support) surface area of the liquid in capillary (eqs 2 and 3):

$$\Delta G = \gamma_{LV}\Delta A^{\text{sphere}} - f(\gamma_{SL}, \gamma_{S'L})\Delta A^{\text{channel}} \quad (1)$$

$$\cong -x\Delta z[3(\gamma_{SV} - \gamma_{SL}) + (\gamma_{S'V} - \gamma_{S'L})] \quad (2)$$

$$\cong -x\Delta z\gamma_{LV}(3\cos\theta^{\text{PDMS}} + \cos\theta^{\text{Support}}) \quad (3)$$

assuming that a liquid filled from a relatively large spherical drop (radius r) into a square capillary (width x). γ_{SV}, γ_{SL}, and γ_{LV} represent solid/vapor, solid/liquid, and liquid/vapor interfacial free energies, respectively. θ^{PDMS} and θ^{Support} correspond to the contact angles of the liquid on the surfaces of PDMS and the support (Figure 1a). Although chemically stable, the PDMS may be affected by its contact with the liquid by swelling (or some other process for reactive liquids). We assume that the polymer surfaces remain unperturbed and homogeneous throughout. The advancing contact angle of the liquid on PDMS (θ_a^{PDMS}) is greater than on the surface of a support ($\theta_a^{\text{Support}}$), since the PDMS has the lower interfacial free energy; the imbibition front advances faster on the support than on PDMS (Figure 1b). When the liquid has a low advancing contact angle on the substrate, its spreading may involve precursor films. After the imbibition front advances to a certain distance, the flow of liquids occurs along the corners formed between the PDMS and support. These corner regions may be connected by thin films of the wetting liquid on the flat regions of the capillary (Figure 1c).

The rate of liquid flow[15,29] in the capillary can be approximated using the surface tension and viscosity of the liquid, the cross-sectional dimension of the capillary, and the length of the channel:

$$\frac{dz}{dt} = \frac{R_H\gamma_{LV}\cos\theta}{4\eta z} = \frac{R_H(\gamma_{SV} - \gamma_{SL})}{4\eta z} \quad (4)$$

where R_H is the hydraulic radius (the ratio between the volume and the surface area of the capillary, e.g., $x^2z/(4xz)$ in cm for a square capillary with width x), η the viscosity (in poise or dyne s/cm^2) of the liquid, and z the length (in cm) of the column of liquid (Figure 1a). The use of the hydraulic radius allows the rate of capillary flow of liquids in square, rectangular, and irregularly shaped capillaries to be approximated. This equation assumes that the insides of the capillary have homogeneous interfacial free energies. The rate of filling is inversely

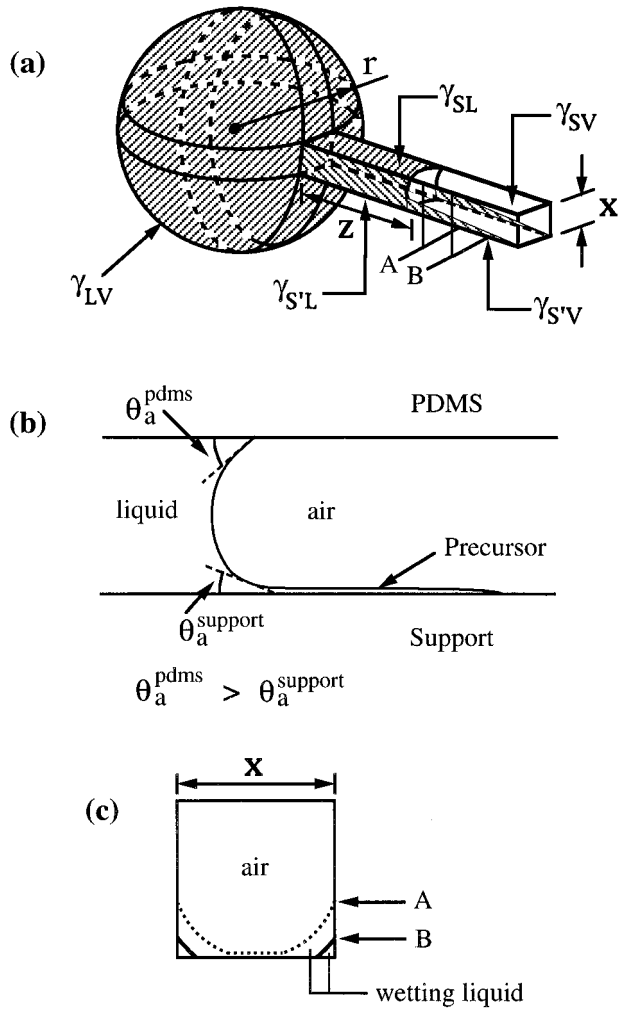

Figure 1. Imbibition of a liquid along the square capillary: (a) model of capillary filling from a liquid spherical drop with radius *r* into a square capillary tube with width *x*; (b) profile depicting the shape of the imbibition front showing different advancing contact angles of the liquid on PDMS and support, with the precursor film preceding the macroscopic flow; (c) views from cross sections A and B in (a), where the cross section from A shows that the liquid imbibes along the corners between the bottom (support) and side surfaces (PDMS) and that the thin film covers the straight regions of the capillary, and the cross section from B shows imbibition along the corners. There is very little imbibition along the corners made of the top (PDMS) and side (PDMS) surfaces.

proportional to the length of capillary that contains the liquid and viscosity of the liquid. The rate of filling decreases as the capillary fills or when a more viscous liquid is used.

Results and Discussion

Rectangular capillaries were filled with a liquid prepolymer using MIMIC. A choice of liquid prepolymer was critical for this procedure to be useful. The liquid prepolymers in this study shared characteristics that allowed the analysis of wetting and imbibition. (1) The liquids were of relatively low viscosity (<400 cP); they filled small capillaries (having cross-sectional dimension of approximately 3−5 μm^2) at a reasonable rate: ~0.4 mm/min for filling channels with 0.5 cm length. (2) They were oligomers of relatively moderate molecular weight (M < ~10^3) and minimized the production of heat during cross-linking. By use of prepolymers with only slightly exothermic cross-linking steps, the accompanying changes in density and distortion in shape were minimized.[30] (3) They were cross-linked photolytically by ultraviolet irradiation. This fast and efficient cross-linking step preserved the shapes of the imbibition front and bulk liquids while cross-linking. (4) They were unreactive toward PDMS. They did not react with, swell, or adhere to the PDMS mold; they preferentially adhered to the surface of the support. Swelling of PDMS by liquid prepolymers was very slight or not observed. The liquid prepolymers that were used successfully included poly(methylacrylate) (SK-9, Summers Optical), epoxies (UV-15 and UV-15-7, Master Bond), and polyurethanes (J-91, Summers; NOA 60, 71, 72, 73, 88, and 113, Norland). The liquid prepolymers that were of low molecular weight (M < ~200) could not be used successfully because they absorbed into and swelled the PDMS. In particular, monomers (e.g., styrene and methyl methacryate) could not be used as the liquid in MIMIC.

Shapes of Imbibition Fronts on Surfaces with Varying Interfacial Free Energy (γ_{SV}). The dynamics of wetting has been studied by varying interfacial free energies of the surface of glass slides using various silanes.[31−33] Studying similar phenomena in small capillaries has been difficult because it has not been practical to vary interfacial free energies in a system of capillaries. In this study, we used self-assembled monolayers (SAMs) of alkanethiolates supported on Au(500 Å)/Ti(10 Å)/SiO_2/Si to control the extent of wetting and spreading of the liquid in rectangular capillaries. We chose to vary the interfacial free energy of the surface (γ_{SV}) of the substrate instead of the interfacial free energy of the liquid (γ_{LV}) because the range of interfacial free energies available in the liquid prepolymers was limited compared to that that could be provided by SAMs. By variation of the structure of the molecular constituents of the alkanethiol, interfacial properties of the surface were controlled over a wide range:[34] alkanethiols with nonpolar headgroups (e.g., CF_3, CH_3) rendered the resulting SAM hydrophobic, and those with polar headgroups (e.g., COOH, OH) rendered the surface hydrophilic.

The shapes of liquids imbibing in the capillaries having different interfacial free energies were observed via microscopy after the shapes had been "frozen" as solid polymers. Scanning electron microscopy (SEM) was useful for observing the shapes of macroscopic fronts, while atomic force microscopy (AFM) was convenient for examination of thin precursor films and small leading edges that moved ahead of the bulk liquid. We looked for different shapes of the liquids on the surface of the substrate (SAM/Au/SiO_2/Si) and the corners made of PDMS and substrate, since the top half of the cross-linked polymer (the shape of the liquid determined by wetting the surface of PDMS and the corners made of PDMS walls) remained constant throughout the experiments. When characterizing and classifying different shapes of imbibing liquids, we used the shape of the bottom half of the cross-linked polymer, since the shape (i.e., the profile of the structure formed on the interface of PDMS and SAM) of the bottom half of the polymer structure was determined by the interfacial free energies of the wetting liquid (γ_{LV}), PDMS (γ_{SV}), and SAM ($\gamma_{S'V}$). Possible shapes[35] of precursor structures include slipping films (with or without shoulders), nonslipping films (wedge or mesa), and plug-flowing films (Figure 2). Slipping films are characterized by "sliding" of the liquid layer along the surface, where the liquid layer spreads freely. This situation corresponds to low advancing contact angles. Some of these slipping films may contain a distinct region (called a "shoulder") that occurs in a region between the macroscopic front and the thin precursor film. Wedge describes the shape of the imbibition front that spreads with a wedge-shaped macroscopic front without a precursor film. This situation corresponds to high advancing contact angles. Mesa corresponds to a special case of "wedge" where a relatively short

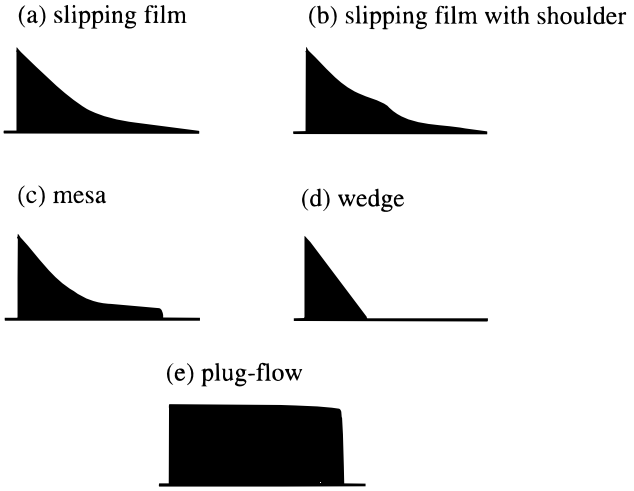

Figure 2. Diagrams representing different shapes of spreading liquids.

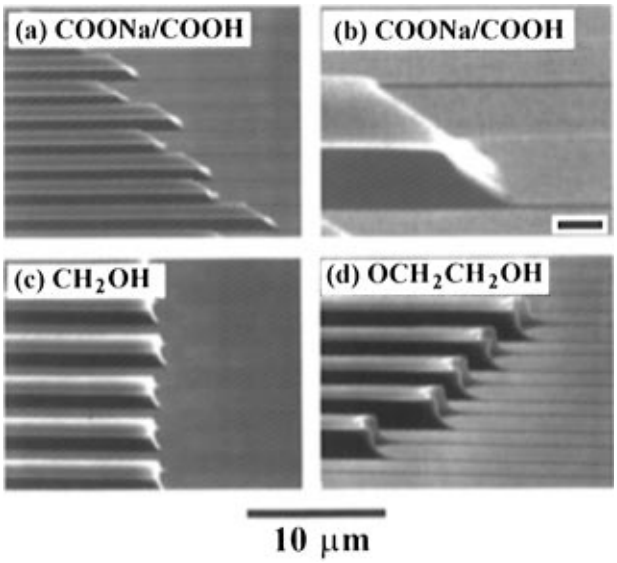

Figure 3. Scanning electron micrographs (SEMs) showing the shape of the imbibing liquids in capillaries formed on hydrophilic SAMs (supported on Au/Ti/SiO_2/Si). All structures were formed from a liquid prepolymer of polyurethane (NOA 73, Summers). The large scale bar at the bottom applies to parts a, c, and d. Part a shows the shape formed on the SAM terminated with COONa/COOH. Thin precursor films precede the macroscopic flow. Part b shows the same structure as in part a at a higher magnification, and the scale bar in the inset corresponds to 1 μm. Part c shows the shape formed on the SAM terminated with OH, and part d shows the shape formed on the SAM terminated with OCH_2CH_2OH.

precursor film precedes the wedge-shaped macroscopic front. A liquid moving in plug-flow refers to a situation in which the entire liquid moves as a whole, without a precursor structure.

Figures 3−7 show scanning electron micrographs (SEMs) and atomic force micrographs (AFMs) of the imbibition front of the liquid in rectangular capillaries formed on hydrophilic, intermediate, and hydrophilic SAMs, as observed as solid polymer (polyurethane) from a liquid prepolymer (NOA 73, Summers Optical; $\eta = 300$ cP, $\gamma_{LV} \approx 39$ dynes/cm[36]), on gold surfaces having different interfacial properties afforded by SAMs having different head groups: −COOH, −OH, $-OCH_2CH_2$-OH, $-C(O)OCH_3$, $-C(O)NHCH_3$, −CN, $-OCH_3$, $-CH_3$, and $-CF_3$. The cross-sectional dimensions of the channels varied from 2.5 μm × 1 μm to 5.0 μm × 1.2 μm. This variance did not seem to affect the shape of the liquid in the capillary.

SAMs with High Interfacial Free Energy. On high free energy, hydrophilic surfaces (e.g., SAM terminated with COOH),

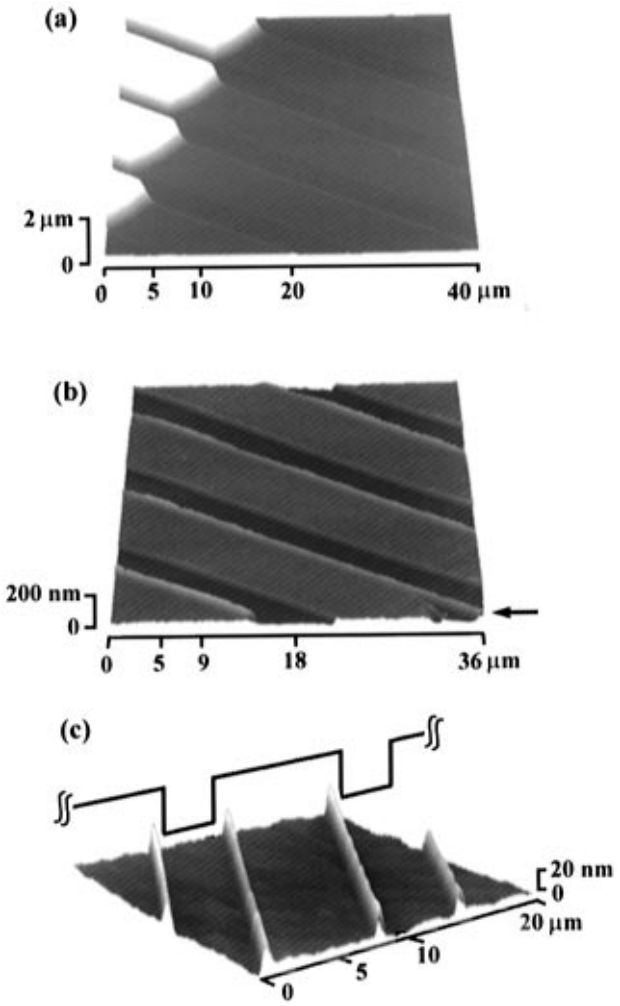

Figure 4. Atomic force micrographs (AFMs) showing the shape of the imbibing liquids (NOA 73) in capillaries formed on the SAM terminated with COONa/COOH. Part a shows the precursor films and macroscopic front. The precursor films are ∼200 nm thick. Part b shows the precursor films in a region ∼4 mm from the macroscopic front. The films here are ∼50 nm thick. On the bottom right of the figure (indicated by an arrow), the precursor film starts to break up into leading edges. Part c shows "leading edge" structures imbibing just ahead of the structures in part b. A schematic drawing of the cross section of the PDMS mold appears above the figure.

the spreading of the liquids showed that thin precursor films preceded the macroscopic flow (parts a and b of Figure 3). The advancing contact angles of the liquid prepolymer on this surface were sufficiently small such that the initial spreading of the liquid occurred through thin films as well as along the corners made of PDMS and SAM. The surface in Figure 3a was made very hydrophilic by washing it with an aqueous solution of NaOH (6 N) and then drying with a vapor of methanol. The surface probably consisted of a mixture of hydrated COO^-Na^+ and COOH groups. Although the shapes of imbibing liquids on the SAMs terminated with COONa/COOH and OH were similar, the precursor films on the SAM terminated with COONa/COOH were more pronounced than on SAM terminated with OH (Figure 3c). As observed by SEM and AFM, a region ahead of the macroscopic front showed the presence of thin, precursor films (∼200−300 nm in thickness in Figures 3b and 4a; less than ∼100 nm in Figure 3c). These thin films extended as far as ∼4−5 mm ahead of the macroscopic front, while the thickness of the film decreased as the distance from the macroscopic front increased. Ahead of these precursor films, there was a region where imbibition occurred along the corners made of PDMS and SAM (Figure 4b); only a small section

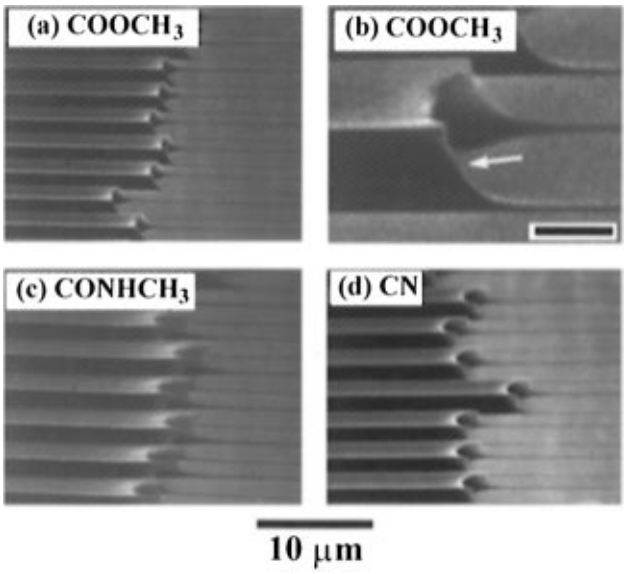

Figure 5. SEMs showing the shape of the imbibing liquids in capillaries formed on moderately hydrophobic SAMs (supported on Au/Ti/SiO_2/Si). All structures were formed from a liquid prepolymer of polyurethane (NOA 73). The scale bar applies to parts a, c, and d. Part a shows the structures formed on the SAM terminated with CO_2CH_3. Part b shows the same as in part a at a high magnification. The scale bar in the inset corresponds to 1 μm. The arrow indicates the "shoulder" (see text for detail). Part c shows the structures formed on the SAM terminated with $CONHCH_3$, and part d shows the structures formed on the SAM terminated with CN.

(~50−100 μm) of the imbibition front showed wicking through the corners. The region indicated by an arrow in Figure 4b shows an area where the thin precursor films break up into these structures showing wicking. These linear structures were approximately 20 nm high and 200 nm wide at the half-height. The shapes (i.e., the profile of the shape formed on the PDMS/SAM/air interface) of imbibing liquids on these surfaces can be classified as slipping films in which low advancing contact angles of the liquid allowed thin precursor films.

Imbibition on the surface composed of the SAM terminated with ethylene glycol (Figure 3d) showed imbibition of the liquid predominately along the corners of the capillary made of PDMS and substrate, although AFM showed the presence of very thin films (less than ~50 nm) on the flat region of the capillary (similar to the structures and shapes shown in Figure 4b). Unlike the structures in parts a−c of Figure 3, these precursor films were sufficiently thin that most imbibition occurred along the corners. The shapes of the imbibition front in Figure 3c may be classified as slipping films with shoulders. These characteristics have been observed in the spreading of polymer melts.[37,38] This special feature of spreading of polymeric liquids has been explained in terms of entanglement of polymeric chains and the consequent gradient in apparent surface shear viscosity.[3,39]

SAMs with Intermediate Interfacial Free Energy. The imbibition and flow of the liquid on surfaces with intermediate interfacial free energies (Figures 5) occurred mostly along the corners of the capillary made of PDMS and substrate. The precursor structures were leading edges resulting from the wetting of the corners made of the PDMS and SAM. Analyses by SEM and AFM revealed that there was no formation of thin precursor films (Figure 6b). Among surfaces with slightly different interfacial free energies (SAMs terminated with CO_2CH_3, $CONHCH_3$, and CN), the shapes of imbibition fronts were similar or indistinguishable. The shapes of the spreading liquid in Figure 5 can be classified as slipping films with shoulders—

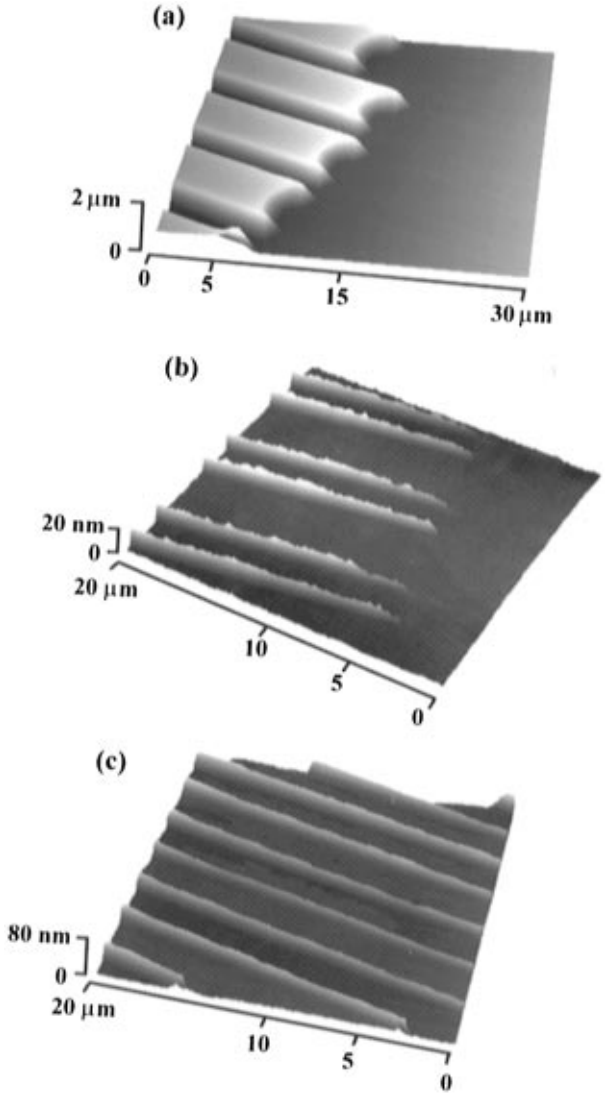

Figure 6. AFMs showing the shape of the imbibing liquids in capillaries formed on the SAM terminated with CO_2CH_3. All structures were formed from a liquid prepolymer of polyurethane (NOA 73). Parts a and b were taken from the same sample and part c from another. Part a shows the macroscopic front and leading edges. Part b shows a region ~700 μm from the macroscopic front, showing the shape of the precursor structure at the beginning of imbibition. The structures do not appear smooth because of exaggerated *z* scale. They are rough only on ~0.1 nm scale. Part c shows a region ~500 μm from the macroscopic front. The structures are approximately 30 nm high and 200 nm wide at the half-height.

regions between the macroscopic front and the precursor structures (indicated by arrow in Figure 5b).

Figure 6 shows an AFM image of the shape of the liquid in capillaries formed on the SAM terminated with CO_2CH_3. These structures were imaged at ~500 μm from the bulk liquid. In Figure 6a, the shape of the macroscopic front does not match perfectly with that shown by SEM in Figure 5a because the cantilever used in AFM could not scan across the large distance in the vertical direction. The AFM shows that the precursor structures were "leading edges" (~30 nm high and 100−150 nm wide at the half-height) that corresponded to imbibition along the corners. We did not observe the formation of thin, precursor films (Figure 6a). Figure 6b shows the region representing the beginning of imbibition. Figure 6c shows a region ~500 μm from the macroscopic front. The leading edges were not connected by films, so far as we can determine using AFM.

SAMs with Low Interfacial Free Energy. Although the interfacial free energy of the SAM terminated with OCH_3 may

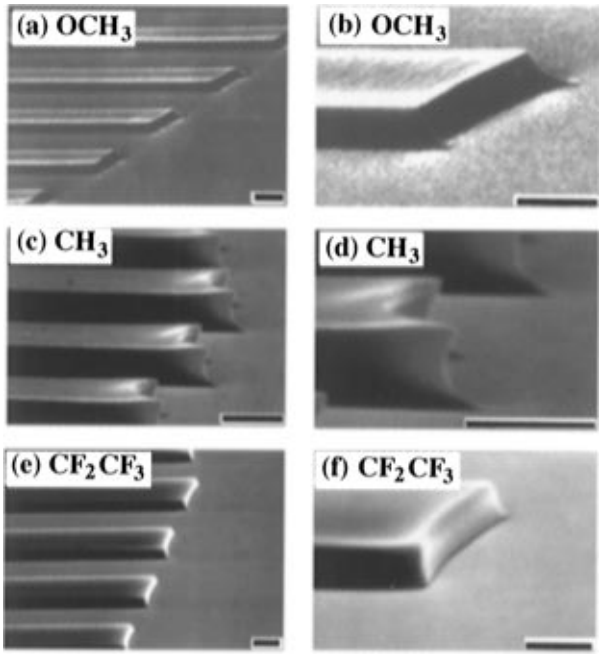

Figure 7. SEMs showing the shape of the imbibing liquids in capillaries formed on hydrophobic SAMs (supported on Au/Ti/SiO_2/Si). All structures were formed from a liquid prepolymer of polyurethane (NOA 73). The scale bar in the bottom right corner of each figure corresponds to 2 μm. Parts a and b show SAM terminated with OCH_3. Part c and d show SAM terminated with CH_3, and parts e and f show SAM terminated with CF_2CF_3.

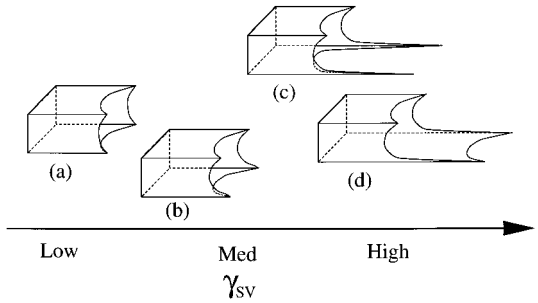

Figure 8. Schematic summary of different spreading regimes observed in MIMIC. Shapes of the imbibing liquids in capillaries are formed on (a) SAMs with γ_{SV}, (b and c) SAMs with medium γ_{SV}, and (d) SAMs with high γ_{SV}.

be classified as moderately hydrophobic, we include this surface here. Figure 7a shows the shape of the imbibition front on the SAM terminated with OCH_3. On this SAM, the precursor structure consisted of short (a few micrometers) leading edges extending ahead of the macroscopic front. There was no other precursor structures in the form of films or leading edges. This shape of imbibition may be classified as mesa (Figure 7b).

The spreading and flow of a liquid in the channels formed on more hydrophobic surfaces (SAMs terminated with CH_3 and CF_2CF_3) showed that the entire macroscopic structure moved as a whole without precursor films or leading edges (parts c−f of Figure 7). Examining one of these structures at a higher magnification (Figure 7f) showed clearly the absence of a precursor structure. High advancing contact angles on theses surfaces did not allow the "slippage" of the liquid on the surface. The shape of the liquid on the SAM terminated with CH_3 may be classified as wedge and on the SAM terminated with CF_2-CF_3 as plug-flow.

Summary of the Shapes of Imbibing Liquids on SAMs with Different γ_{SV}. Figure 8 and Table 1 summarize the shapes of imbibing liquids in capillaries having different interfacial free energies. Two related parameters that control the shape of spreading liquid are the advancing contact angle (θ_a) and the interfacial free energy of the surface (γ_{SV}). We observe three different regimes of spreading liquids in MIMIC. (1) For the liquids with small advancing contact angles (i.e., high γ_{SV}), the imbibition fronts can be characterized as slipping films. (2) For the liquids with intermediate advancing contact angles (i.e., medium γ_{SV}), the shapes of the imbibition fronts consist of leading edges that have resulted from preferential wetting of the corners made of the PDMS and substrate. These shapes can be considered as slipping films with shoulders, and (3) for the liquids with high advancing contact angles (i.e., low γ_{SV}), the bulk liquid spreads as a whole without having precursor structures. These shapes can be characterized as wedge or bulk-flow.

TABLE 1: Summary of the Shapes of Imbibing Liquids in Square Capillaries Having Different Interfacial Free Energies

shape[a]	interfacial free energy (γ_{SV})[b]	leading edges[c]	precursor films
a	low	no	no
b	low/med	short	no
c	med	yes	no
d	high	yes	yes

[a] Shapes correspond to the structures diagramed in Figure 8. [b] Interfacial free enegies of the surfaces were varied using SAMs supported on Au/Ti/SiO_2/Si. [c] "Leading edges" refer to the linear structures that advanced ahead of the macroscopic flow and that resulted from preferential wetting of the corners made of PDMS and SAM.

Imbibition and Flow through Channels Having Complex Geometry. Figure 9 shows SEMs of imbibition and flow of a liquid through the channels in a complex pattern. The liquid was a prepolymer of polyurethane (J-91, Summers), and the substrate was gold functionalized with a SAM having carboxylic acids as its head groups. It was subsequently washed with an aqueous solution of NaOH (6 N) and dried with a vapor of methanol just before the use. From imbibition and flow of the liquid through the capillary having complex geometry, we observed that (1) as in the imbibition through capillaries with simple geometry, precursor films preceded the macroscopic flow when the advancing contact angle of the liquid was low (Figure 9a) and (2) as the liquid filled the capillaries, it preferentially filled the corners of the capillaries (made of the PDMS and SAM) and the edges of the pattern (e.g., the interconnected triangular patterns in the figure). In a region where capillary filling is in progress (Figure 7b), the liquid wets the edges in the pattern preferentially and fills these regions faster than other regions. These observations can be explained in terms of balances in interfacial free energies of liquid/vapor, solid/vapor, and solid/liquid. First, precursor films spread to maximize the interfacial surface area of the liquid and the high energy surface (the SAM terminated with COONa/COOH) and to minimize the surface area of the SAM/air interface. Then the liquid flows to maximize the surface area of the liquid/PDMS interface and to minimize the surface area of liquid/vapor interface.

Dependence of Rates of Imbibition on the Interfacial Free Energy of the Surface. The rate of imbibition is related to the interfacial free energy of the surface by the contact angle of the liquid on the surface (eq 4). The contact angle of the liquid must be small enough to allow imbibition. For a system using a specific geometry of the capillary and a liquid, the rate of the capillary flow is a function of cos θ_a, since R_H (hydraulic radius, the ratio of the volume of liquid to the surface area of the volume) and γ_{LV}/η are constant for this system. Table 2 lists static advancing (θ_a) and receding (θ_r) contact angles of the liquid prepolymer of polyurethane (NOA 73) on SAMs

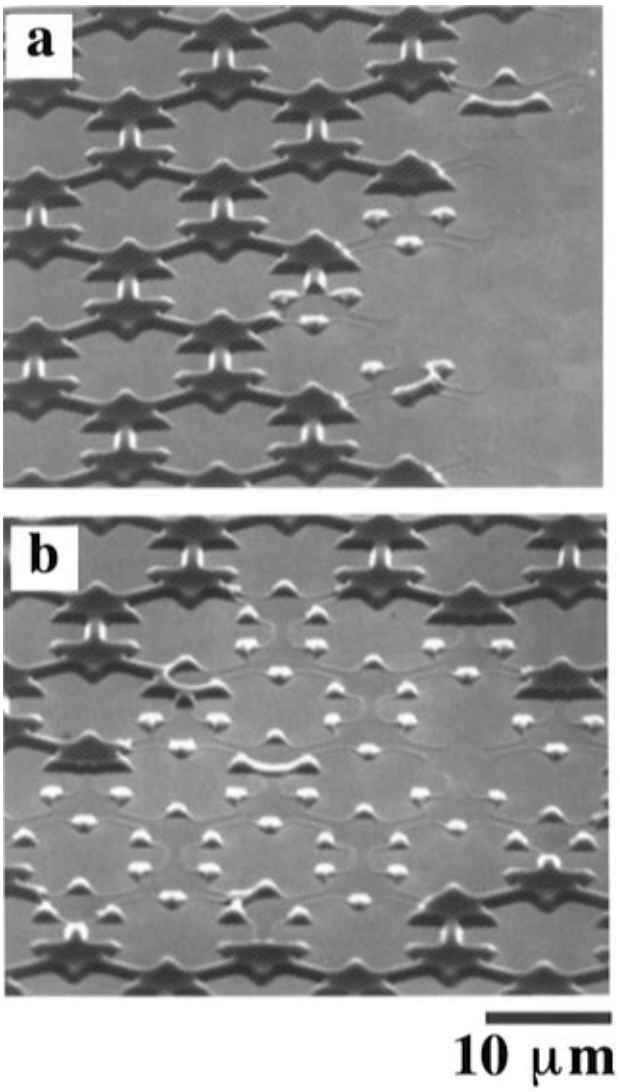

Figure 9. Imbibition and flow of a liquid prepolymer of polyurethane (J-91, Summers) through capillaries having complex shapes and complex patterns. Part a shows an SEM of a region where the liquid starts to fill the capillaries. Although thin precursor films extend ahead of the macroscopic flow, some imbibition occurs along the corners formed between the PDMS and support. These corners appear as ridges that are 2−4 times thicker than the precursor films. Part b shows an SEM of a region where the liquid has not filled completely. The progression of imbibition shows the preferential wetting of corners of the capillary and edges of the pattern.

having different functional groups and on a film of PDMS. Table 2 shows that the advancing contact angle on PDMS is higher than most of the surface that we used; the liquid prepolymer preferentially wets the support rather than the PDMS mold.[40] This observation agrees with our previous observations.[15]

We observed viscoelastic dissipation[41]—spreading of a liquid being affected by a sufficiently soft solid that forms a local deformation near the wetting front and impedes the further wetting and spreading—in our systems because one of the components of the capillary was an elastomer. Dynamic advancing contact angles (θ_a^d) of the liquid on the PDMS wall in the capillary were much higher than the static contact angle (θ_a^s): $65° \leq \theta_a^d \leq 104°$ and $\theta_a^s = 58 \pm 3°$. The greatest viscoelastic effect occurred at the interface between PDMS and liquid, but this phenomena seemed to occur at all interfaces involving PDMS/SAM/liquid. Owing to the preferential wetting of the rigid support (i.e., SAM) by liquids rather than the elastomeric PDMS, we did not consider the effect of viscoelastic dissipation in our system.

TABLE 2: Static Advancing and Receding Contact Angles of a Liquid Prepolymer of Polyurethane (NOA 73, Norland) on a Film of PDMS and Surfaces Prepared by Adsorption of $HS(CH_2)_nX$ on Gold

		contact angles (deg)[a]	
n	surface[b]	advancing (θ_a)	receding (θ_r)
	PDMS	58	42
2	$-CF_2CF_3$	74	56
15	$-CH_3$	61	38
11	$-OCH_3$	39	15
10	$-COOCH_3$	32	–
11	$-CONHCH_3$	31	–
11	$-CN$	25	–
11	$-OCH_2CH_2OH$	20	–
16	$-OH$	17	–
11	$-COONa/COOH$[c]	<15	–

[a] A dash indicates that the contacting liquid could not be removed from the surface while measuring receding contact angles. The reproducibility in the values of θ is about ±3°. [b] Surfaces were a film of PDMS (Sylgard 184, Dow Corning) and SAMs on gold functionalized with alkanethiols having the listed head groups and chain lengths. [c] This surface was prepared by washing the SAM terminated with COOH with an aqueous solution of NaOH (6 N) and drying it with a vapor of methanol.

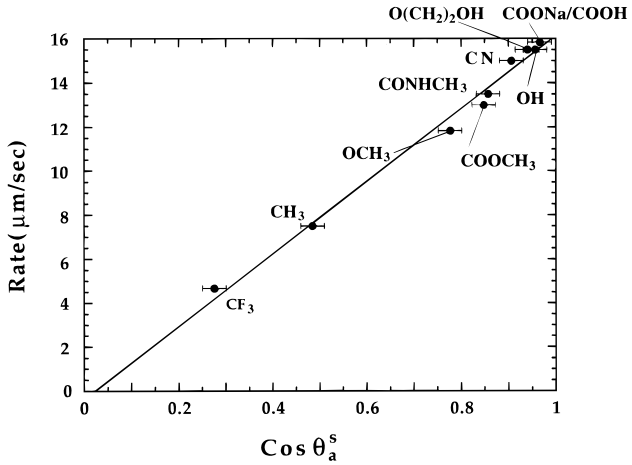

Figure 10. Plot of initial rate of capillary filling vs the cosine of the static advancing contact angles ($\cos \theta_a^s$). See text for details. A linear curve fits the data well with a slope of 1.63×10^{-3} and a *y* intercept of -2.12×10^{-5}. Error bars indicate experimental uncertainties in values of advancing contact angles.

Equation 4 predicts a linear relationship between the rate of imbibition and the cosine of the advancing contact angles ($\cos \theta_a$). Figure 10 shows that this prediction is observed. The initial rates were measured as the time it took for the macroscopic front of the liquid to fill the first 2 mm of the capillary. The initial rate of imbibition was used, since the rate decreased as the distance from the imbibition front to the origin increased. If liquids travel a large distance in capillaries, the rate of filling decreases inversely with respect to the distance it has filled (eq 4), and eventually, the average rates of filling capillaries formed on different SAMs become similar because of viscous drag. Using initial rates ensured that the contribution due to interfacial free energy predominated in the kinetics of imbibition, since *z* and η were constant for each rate. When only a short distance was filled, however, the interfacial free energies seemed to be the dominant contributors to the spreading velocity.

The data fit a linear plot well, with a *y* intercept of -2.12×10^{-5} and a slope of 1.63×10^{-3}. From the slope, R_H (hydraulic radius) was calculated to be 1.00×10^{-4} cm (or about 1 μm) using $\gamma_{LV} = 39$ dyne/cm,[35] $\eta = 3.0$ poise (dyne s/cm^2), and $z = 0.2$ cm. From the geometry of the capillary and the definition

of hydraulic radius (see Theory section), R_H is expected to be 0.44×10^{-4} cm, assuming a capillary cross section of 1.75×1.75 μm (~ 3 μm^2). This discrepancy supports the well-known contention that the hydraulic-radius approximation can introduce large errors when applied to capillary-flow problems in noncircular tubes.[42]

Although the data fit a linear relationship well, there are uncertainties in the experimental procedure that cloud the interpretation. (a) We treated the liquid prepolymer as a simple liquid. In reality, however, this liquid consists of oligomers, cross-linking reagents, and photoinitiators. The effect of using the polymeric mixture on the dynamics of wetting and spreading is ambiguous. (b) Another uncertainty in our system is the effects of contamination from the ambient atmosphere on the interfacial properties of the surfaces. Adsorption of water and pollutants from the atmosphere may have played a significant role in the balances of interfacial free energies.

Dependence of Rates of Imbibition on the Dynamic Advancing Contact Angles. We measured *static* advancing contact angles of millimeter-scale drops and used them in an analysis that involved *dynamic* advancing contact angles[43,44] in micrometer dimensions (Figure 10). Dynamic contact angles give average values, which need not correspond to those in equilibrium. Static contact angles are more sensitive to local heterogeneity and are equilibrium parameters. The relationship observed in Figure 10 suggests that, in our experimental conditions, static contact angles approximated dynamic contact angles well.

Since our experimental protocol made it possible to obtain dynamic structures of the liquids in the capillary, we obtained dynamic contact angles of the liquid advancing in the capillaries formed on the SAM terminated with CF_2CF_3 by measurements taken from the cross-linked, solid polymers. We chose this system involving a highly hydrophobic surface for several useful characteristics: (1) the liquid prepolymer has the highest static advancing contact angles (Table 2) on this SAM, and this high value provides the maximum to which dynamic contact angles may be varied; (2) the low interfacial free energy means that the contamination from the ambient sources is minimal; (3) the rate of capillary filling is slow enough that it is practical to fill only a small portion of the capillary; (4) the advancing contact angles are high enough that they could be measured accurately from the cross-linked polymers.

Dynamic contact angles of the liquid prepolymer (NOA 73) were measured in different regions of capillary (i.e., at different distances from the origin). We filled the capillary to the desired distance, which varied from 10 μm to 5 mm, cross-linked the liquid prepolymer by UV irradiation, and determined the contact angle of the liquids on the SAM by examination of the solid polymers. We observed that the value of the observed advancing contact angle approached the equilibrium value at $z \geq 4$ mm from the origin of imbibition. When the liquid filled the capillary to less than this distance, the shape in the capillary represented dynamic structures, and $\theta_{observed}$ was less than $\theta_{equilibrium}$.

Figure 11 shows the plot of the cosine of *dynamic* advancing contact angles ($\cos \theta_a^d$) vs the product ($z(dz/dt)$) of the rate of capillary imbibition and the length of capillary filling, and the shape of the liquid corresponding to each point on the plot.

These shapes (insets in Figure 11) showed different values of θ_a^d because the velocity of liquid flow affected these angles. At different distances from the origin of imbibition, the liquid moved at different velocities because of the inverse relationship between the rate of imbibition and the distance of the capillary filling (eq 4). At a short distance relative to the origin (i.e., small z), θ_a^d was smaller than that at large z. The shapes of liquids in Figure 11 confirms our observation that spreading at small θ_a involves precursor structures and that there are no precursor structures for spreading at large θ_a. As the liquid filled the capillaries, the dynamic contact angles approached the static contact angle. The data in Figure 10 fitted a linear relationship because we obtained the rate of capillary imbibition from the regime very close to the equilibrium.

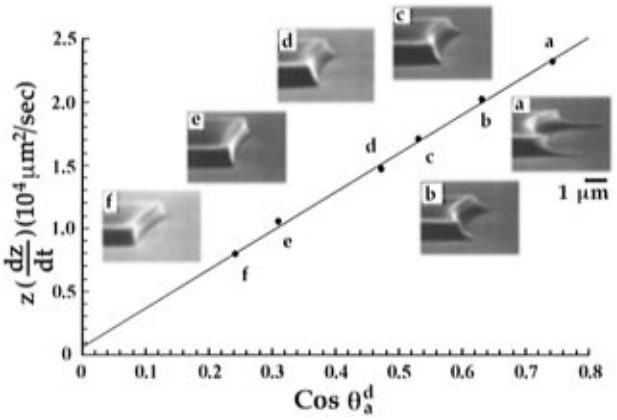

Figure 11. Plot of $z(dz/dt)$ vs $\cos \theta_a^d$. We determined the advancing contact angles from the SEMs taken at difference lengths of capillary imbibition: (a) 10 μm; (b) 100 μm; (c) 0.5 mm; (d) 1 mm; (e) 2 mm; and (f) 4 mm.

Conclusions

We have studied imbibition and flow of liquids in rectangular capillaries by characterizing the dynamic shapes of the liquids cross-linked to solids. Different regimes of spreading in capillaries occur as the liquid in the capillary experiences differences in the balance of interfacial free energies. Self-assembled monolayers (SAMs) are excellent tools with which to control the interfacial characteristics of the inside of the capillary. On surfaces with high γ_{SV} (e.g., SAMs terminated with COOH and OH), precursor films precede the macroscopic flow. On surfaces with low γ_{SV} (e.g., SAMs terminated with CH_3 and CF_3), the macroscopic front of the liquid advances as a whole without having a precursor structure. On surfaces with intermediate γ_{SV} (e.g., SAMs terminated with $COOCH_3$, CN, and OCH_3), different precursor structures may precede the macroscopic flow. Some of these structures include slipping films, shoulder, and mesa.

The rate of capillary imbibition is directly proportional to the cosine of static advancing contact angles of the liquid on the wetting surface. Liquids with low advancing contact angles fill the capillary faster than those with higher advancing contact angles. When the rate of capillary imbibition is low, precursor structures (films or edges) are absent; precursor structures are present when imbibition is fast.

In the same way that different regimes of spreading can be observed on surfaces of varying γ_{SV}, related regimes can be observed with differences in the velocity of the imbibition (eq 4) on surface of constant γ_{SV}. As a liquid moves along capillaries that have low γ_{SV}, it experiences different regimes of spreading: from high-slip regimes (when z is small and dz/dt is large) to no-slip regimes (when z is large and dz/dt is small).

Wetting and spreading of liquids in MIMIC is a problem that involves relatively viscous liquids that partially wet noncircular capillaries having sides with different interfacial free energies. This system provides an excellent model for studying the dynamics of imbibing liquids in rectangular capillaries in which interfacial characteristics of capillaries and imbibing liquids can

be varied systematically. By photopolymerization of the liquid prepolymers, the dynamic structures of imbibing liquids determined by interfacial free energies can be "frozen" inside the capillary and fine details of the shapes can be examined via microscopy. It is unclear to us what artifacts in this shape are introduced by our experimental protocol that involves elastomeric mold, polymeric liquids, and photopolymerization. Nevertheless, this system of "demountable capillaries" formed between the mold and surface, along with its simple experimental procedures, is a convenient one for examining capillary filling.

Acknowledgment. This work was supported in part by the Office of Naval Research, the Advanced Research Projects Agency, and the ARO Multidisciplinary University Research Initiative (DAAH04-95-1-0102). It used MRSEC Shared Facilities supported by the National Science Foundation (DMR-9400396).

References and Notes

(1) Hoffman, R. L. *J. Colloid Interface Sci.* **1975**, *50*, 228.
(2) Hoffman, R. L. *J. Colloid Interface Sci.* **1983**, *94*, 470.
(3) de Genne, P. G. *Rev. Mod. Phys.* **1985**, *75*, 827.
(4) Heertjes, P. M.; Witvoet, W. C. *Powder Technol.* **1969**, *3*, 339.
(5) Vizika, O.; Payatakes, A. C. *PCH, PhysicoChem. Hydrodyn.* **1989**, *11*, 787.
(6) Defay, R.; Prigogine, I. *Surface Tension and Absorption*; Wiley: New York, 1966; p 217.
(7) Arriola, A.; Willhite, G. P.; Green, D. W. *Soc. Pet. Eng. J.* **1983**, *23*, 99.
(8) Schwartz, A. M. In *Surface and Colloid Science*; Matijevic, E., Ed.; Wiley-Interscience: New York, 1972.
(9) Legait, B. *J. Colloid Interface Sci.* **1983**, *96*, 28.
(10) Ransohoff, T. C.; Radke, C. J. *J. Colloid Interface Sci.* **1988**, *121*, 392.
(11) Mason, G.; Morrow, N. R. *J. Colloid Interface Sci.* **1991**, *141*, 262.
(12) Dong, M.; Chatzis, I. *J. Colloid Interface Sci.* **1995**, *172*, 278.
(13) Dong, M.; Dullien, F. A.; Chatzis, I. *J. Colloid Interface Sci.* **1995**, *172*, 21.
(14) Zasadzinski, J. A.; Sweeney, J. B.; Davis, H. T.; Scriven, L. E. *J. Colloid Interface Sci.* **1987**, *119*, 108.
(15) Kim, E.; Xia, Y.; Whitesides, G. M. *Nature* **1995**, *376*, 581.
(16) Kim, E.; Xia, Y.; Whitesides, G. M. *J. Am. Chem. Soc.* **1996**, *118*, 5722.
(17) Xia, Y.; Kim, E.; Whitesides, G. M. *Chem. Mater.* **1996**, *8*, 1558.
(18) Kim, E.; Xia, Y.; Whitesides, G. M. *Adv. Mater.* **1996**, *8*, 245.
(19) *Introduction to Microlithography*; Thompson, L. F., Wilson, C. G., Bowden, M. J., Eds.; ACS Symposium Series 219; American Chemical Society: Washington, DC, 1983.
(20) Elliott, D. J. *Integrated Circuit Fabrication Technology*; McGraw-Hill: New York, 1982.
(21) Wilbur, J. ; Kim, E.; Xia, Y.; Whitesides, G. M. *Adv. Mater*. **1995**, *7*, 649.
(22) The transmission efficiency is greater than 80% for $\lambda > 400$ nm for a 2.54 mm thick film. Technical Report No. Q3-6696; Dow Corning: Midland, MI, 1991.
(23) Kim, E.; Kumar, A.; Whitesides, G. M. *J. Electrochem. Soc*. **1995**, *142*, 628.
(24) Bain, C. D.; Troughton, E. B.; Tao, Y.; Evall, J.; Whitesides, G. M.; Nuzzo, R. G. *J. Am. Chem. Soc.* **1989**, *111*, 321.
(25) Kumar, A.; Whitesides, G. M. *Appl. Phys. Lett.* **1993**, *63*, 2002.
(26) Kumar, A.; Biebuyck, H. A.; Whitesides, G. M. *Langmuir* **1994**, *10*, 1498.
(27) Bain, C. D.; Evall, J.; Whitesides, G. M. *J. Am. Chem. Soc.* **1989**, *111*, 7155.
(28) Laibinis, P. E.; Whitesides, G. M. *J. Am. Chem. Soc.* **1992**, *114*, 1990.
(29) Myers, D. *Surfaces, Interfaces, and Colloids*; VCH Publishers: New York, 1991; p 87.
(30) The effect of cross-linking on the shape of a macroscopic drop was observed directly by polymerizing an unconstrained, macroscopic drop of the liquid prepolymer by UV irradiation. The liquid retained the shapes of the drop and the accompanying precursor structures.
(31) Elliott, G. E.; Riddiford, A. C. *J. Colloid Interface Sci.* **1967**, *23*, 389.
(32) Sedev, R. V.; Petrov, J. G. *J. Colloid Interface Sci.* **1992**, *62*, 141.
(33) Johnson, R. E., Jr.; Dettre, R. H.; Brandreth, J. A. *J. Colloid Interface Sci.* **1977**, *62*, 205.
(34) For a review on SAMs see the following. Dubois, L. H.; Nuzzo, R. G. *Annu. Rev. Phys. Chem.* **1992**, *43*, 437.
(35) de Genne, P. G. In *Liquids at Interfaces*; Charvolin, J., Joanny, J. F., Zinn-Justin, J., Eds.; North-Holland: Amsterdam, 1988; p 311.
(36) Miller, R. In *Polymer Handbook*, 3rd ed.; Bradrup, J., Immergut, E. H., Eds.; Wiley-Interscience: New York, 1989; p VI-422.
(37) Schonhorn, H.; Frisch, H. L.; Kwei, T. K. *J. Appl. Phys.* **1966**, *37*, 4967.
(38) Ogarev, V.; Timonia, T.; Arslanov, V.; Trapeznikov, A. *J. Adhes.* **1974**, *6*, 337.
(39) Brochard, F.; de Genne, P. G. *J. Phys. Lett. (Paris)* **1984**, *45*, L597.
(40) Even on the SAMs terminated with CH_3 and CF_2CF_3, we did not encounter a problem of delamination of the polymer structures when the PDMS mold was removed. There are possible sources of this adhesion: (1) although the adhesion of the polymer on the surface of PDMS may be favored thermodynamically, the local deformation of the PDMS surface during the removal of the PDMS may have caused the polymer to remain on the SAM; (2) the polymer structures adhered strongly to the surface at the defect sites in the SAM, and these microscopic attachments translated into the macroscopic adhesion of the polymer.
(41) Shanahan, M. E. R.; Carre, A. *Langmuir* **1995**, *11*, 1396.
(42) Bird, R. B.; Stewart, W. E.; Lightfoot, E. N. *Transport Phenomena*; Wiley: New York, 1960; p 204.
(43) Petrov, P. G.; Petrov, J. G. *Langmuir* **1995**, *11*, 3261.
(44) Sedev, R. V.; Budziak, C. J.; Petrov, P. G.; Neumann, A. W. *J. Colloid Interface Sci.* **1993**, *159*, 392.